

Article

---

# Local Quantum Uncertainty and Quantum Interferometric Power in an Anisotropic Two- Qubit System

---

Nour Zidan, Atta Ur Rahman, Saeed Haddadi, Artur Czerwinski and Soroush Haseli

Special Issue





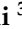
Theories and Applications of Quantum Entanglement

Edited by  
Prof. Dr. Yu Shi



## Article

# Local Quantum Uncertainty and Quantum Interferometric Power in an Anisotropic Two-Qubit System

Nour Zidan <sup>1</sup>, Atta Ur Rahman <sup>2</sup>, Saeed Haddadi <sup>3,4,\*</sup>, Artur Czerwinski <sup>5</sup> and Soroush Haseli <sup>3,6</sup>

- <sup>1</sup> Mathematics Department, College of Science, Jouf University, Sakaka P.O. Box 2014, Saudi Arabia  
<sup>2</sup> School of Physics, University of Chinese Academy of Sciences, Yuquan Road 19A, Beijing 100049, China  
<sup>3</sup> School of Physics, Institute for Research in Fundamental Sciences (IPM), Tehran P.O. Box 19395-5531, Iran  
<sup>4</sup> Saeed's Quantum Information Group, Tehran P.O. Box 19395-0560, Iran  
<sup>5</sup> Institute of Physics, Faculty of Physics, Astronomy and Informatics, Nicolaus Copernicus University in Torun, ul. Grudziadzka 5, 87-100 Torun, Poland  
<sup>6</sup> Faculty of Physics, Urmia University of Technology, Urmia 57166-93188, Iran  
\* Correspondence: saeed@ssqig.com

**Abstract:** Investigating the favorable configurations for non-classical correlations preservation has remained a hotly debated topic for the last decade. In this regard, we present a two-qubit Heisenberg spin chain system exposed to a time-dependent external magnetic field. The impact of various crucial parameters, such as initial strength and angular frequency of the external magnetic field along with the state's purity and anisotropy of the spin-spin on the dynamical behavior of quantum correlations are considered. We utilize local quantum uncertainty (LQU) and quantum interferometric power (QIP) to investigate the dynamics of quantum correlations. We show that under the critical angular frequency of the external magnetic field and the spin-spin anisotropy, quantum correlations in the system can be successfully preserved. LQU and QIP suffer a drop as the interaction between the system and field is initiated, however, are quickly regained by the system. This tendency is confirmed by computing a measure of non-classical correlations according to the Clauser–Horne–Shimony–Holt inequality. Notably, the initial and final preserved levels of quantum correlations are only varied when variation is caused in the state's purity.

**Keywords:** non-classical correlations; local quantum uncertainty; quantum interferometric power; Bell-nonlocality; CHSH inequality; quantum entanglement



**Citation:** Zidan, N.; Rahman, A.U.; Haddadi, S.; Czerwinski, A.; Haseli, S. Local Quantum Uncertainty and Quantum Interferometric Power in an Anisotropic Two-Qubit System. *Universe* **2023**, *9*, 5. <https://doi.org/10.3390/universe9010005>

Academic Editor: Fernando Sols

Received: 9 November 2022

Revised: 16 December 2022

Accepted: 16 December 2022

Published: 21 December 2022



**Copyright:** © 2022 by the authors. Licensee MDPI, Basel, Switzerland. This article is an open access article distributed under the terms and conditions of the Creative Commons Attribution (CC BY) license (<https://creativecommons.org/licenses/by/4.0/>).

## 1. Introduction

Non-classical correlations are currently the primary focus of foundational research in the developing field of quantum information science [1]. Quantum entanglement, which describes a specific type of non-classical correlation between quantum subsystems, has become a critical resource [2,3]. Besides, entanglement has recently been generated from physical systems in quantum gravity [4], quantum fields [5], and condensed matter designs [6]. Recently, in many-body physics, optical lattice structures were found to contain experimental proof of quantum entanglement between their sub-particles [7]. The fundamental distinction between quantum and classical physics in many-body systems is provided by the existence of a quantum correlation between them. However, geometric quantum discord [8,9], measurement-induced non-locality (MIN) [10], measurement-induced disturbance [11], and so on are new types of quantum correlations that have emerged beyond quantum entanglement and need to be correctly characterized in quantum systems of interest.

The development of methods to measure these quantum correlations also remained a difficult problem in quantum information sciences and the conception of techniques to assess these non-classical correlations is still a challenging issue. As a result, local quantum

uncertainty (LQU), a modified version of MIN, was developed, which is one of the non-classical correlation measures with high computability power [12]. LQU captures strictly non-classical correlations without computing their classical equivalent. This quantum discord-type measure has the advantage that LQU estimations do not need to go through the time-consuming optimization process. LQU also meets every condition outlined by a qualified quantum correlations quantifier [13,14]. Determining the level of measurement uncertainty for an observable is based on the Skew information idea, which was initially put forward by Wigner [13,14]. The LQU measure has the advantage of being analytically quantifiable for qubit-qudit systems [15]. The parallel between this unique quantum correlation quantifier and quantum Fisher information (QFI), which is frequently used in the context of quantum metrology, is particularly intriguing [16–18].

Quantum interferometric power (QIP), newly presented in Ref. [19] as a descriptor of quantum correlations, may be used to examine the impact of non-classical correlation in enhancing the accuracy of quantum metrology procedures. One of the reliable measures of correlations that resemble quantum discord is the QIP measure [20]. The degree of accuracy that a bipartite state offers to ensure the achievement of the estimation process irrespective of the phase direction is inherently connected to the QIP since, it is described in terms of QFI [21]. In general, QFI is used to generate the QIP, which may have a variety of intriguing properties [22,23]. The QFI, for instance, is positive, remains invariant to local unitary transformations, does not expand when classical operations are applied to the second qubit, and is asymmetric with regard to the two sub-components unless symmetric quantum states are involved [24,25].

The Heisenberg Hamiltonians have the integrable ability to precisely characterize the spectrum of the involved systems [26–28]. This framework, which Heisenberg first suggested it in 1928 [29], can be viewed as the paradigmatic example of a significant class of integrable structures in low dimensions in both classical and quantum statistical mechanics as well as field theory. In practice, they have been put to use in a variety of fields, such as high-energy physics and condensed matter physics [30–33]. Besides, in recent years, a strenuous effort has been made to investigate Heisenberg spin chains and significant results have been achieved in the case of quantum correlations preservation [10,33–43]. Notably, the reduced density matrix of the spin-1 Heisenberg chains has been examined using the techniques of quantum information theory, including by examining quantum mutual information, quantum discord, entropic uncertainty relations, and three different coherence measurements [44,45]. In contrast to the entanglement of formation and other thermodynamic properties, quantum discord has been used to highlight the key sites connected with quantum phase transitions for the XXZ Heisenberg spin chain model [46]. It is demonstrated that these tendencies are distinct from those of thermal entanglement and the thermal quantum correlations can be produced by adjusting the external magnetic field and the Heisenberg coupling value of the antiferromagnetic system [47]. Other examples of generating and preserving quantum correlations in Heisenberg spin chains can be found in Refs. [48–50].

In this work, we consider an anisotropic two-qubit Heisenberg XY model subject to a time-dependent external magnetic field. In particular, we are interested in quantifying the degree of preserved quantum correlations in a two-qubit Heisenberg spin chain model. Besides, we provide the impact of spin-spin coupling strength, anisotropy of the spin-spin parameters, and frequency of the external magnetic field on the quantum correlations preservation strength of the Heisenberg spin chain. For this purpose, we utilize LQU and QIP measures to quantify quantum correlations in the mentioned system. In addition, we aim to draw a comparison of LQU and QIP measures with Bell-nonlocality violation parameter.

We organize this work as follows. In Section 2, we discuss the quantum correlations criteria and related mathematical quantification. Section 3 illustrates the physical model of the system and in Section 4, the main results obtained for the system are disclosed. The

analysis of quantum correlations with the Bell-nonlocality violation is given in Section 5. Finally, in Section 6, some concluding remarks are provided.

### 2. Local Quantum Uncertainty and Quantum Interferometric Power

We start with a short overview of LQU and QIP. Indeed, LQU is a quantum discord-like criterion of quantum correlations suggested by Girolami et al. [13]. It measures the minimal quantum uncertainty in a considered quantum state because of the measurement of any local observable. For a bipartite quantum state such as  $\rho_{AB}$ , the LQU is described as

$$\text{LQU} = \min_{H_A} \text{I}(\rho_{AB}, H_A \otimes I_B), \tag{1}$$

where  $\text{I}(\rho_{AB}, H_A \otimes I_B) = -\frac{1}{2} \text{Tr} \left\{ \left[ \sqrt{\rho_{AB}}, H_A \otimes I_B \right]^2 \right\}$  is the skew information denoting non-commutation between the quantum state  $\rho_{AB}$  and the operator  $H_A$ , which is indeed an Hermitian operator acting on the subsystem  $A$  and  $I_B$  is the common identity operator acting on the subsystem  $B$ . It is worth mentioning that the LQU is a genuine quantifier of quantum correlations, and it has been shown that the LQU meets all the physical conditions of a criterion of quantum correlations [13]. For any bipartite  $2 \otimes d$  quantum systems, the analytical formula of the LQU is presented as

$$\text{LQU} = 1 - \lambda_{\max}[W_{AB}], \tag{2}$$

where  $\lambda_{\max}[W_{AB}]$  is the largest eigenvalue of the  $3 \times 3$  matrix  $W_{AB}$  whose matrix elements are defined by

$$(W_{AB})_{ij} = \text{Tr} \left\{ \sqrt{\rho_{AB}} \left( \sigma_A^i \otimes I_B \right) \sqrt{\rho_{AB}} \left( \sigma_A^j \otimes I_B \right) \right\}, \tag{3}$$

where  $\sigma_A^i$  and  $\sigma_A^j$  represent the Pauli operators of subsystem  $A$  with  $i(j) = \{x, y, z\}$ .

Alternatively, Gibilisco et al. [14] have also introduced another computable measure of discord-type quantum correlations named as QIP, which is defined as the QFI over all local Hamiltonians  $H_A$  acting on part  $A$

$$\text{QIP} = \frac{1}{4} \min_{H_A} F(\rho_{AB}, H_A), \tag{4}$$

where the minimum  $F(\rho_{AB}, H_A)$  denotes the QFI with local Hamiltonians  $H_A$  acting on part  $A$  defined as [51,52]

$$F(\rho_{AB}, H_A) = \frac{1}{2} \sum_{i,j:p_i+p_j \neq 0} \frac{(p_i - p_j)^2}{p_i + p_j} \left| \langle \psi_i | H_A \otimes I_B | \psi_j \rangle \right|^2, \tag{5}$$

with  $\{p_i, \psi_i\}$  being, respectively, the eigenvalues and eigenstates of  $\rho_{AB} = \sum_i p_i |\psi_i\rangle \langle \psi_i|$ . To minimize  $F(\rho_{AB}, H_A)$ , one can take the local Hamiltonian as  $H_A = \vec{\sigma} \cdot \vec{r}$  with  $|\vec{r}| = 1$  and  $\vec{\sigma} = (\sigma^x, \sigma^y, \sigma^z)$ . From this calculation, a closed formula for QIP of an arbitrary quantum state of a bipartite system is obtained as [14,20]

$$\text{QIP}(\rho_{AB}) = \lambda_{\min}[M], \tag{6}$$

where  $\lambda_{\min}[M]$  denotes the smallest eigenvalue of the symmetric matrix  $M$  whose matrix elements are defined as follows [20]

$$M_{lk} = \frac{1}{2} \sum_{i,j:p_i+p_j \neq 0} \frac{(p_i - p_j)^2}{p_i + p_j} \langle \psi_i | \sigma_A^l \otimes I_B | \psi_j \rangle \langle \psi_j | \sigma_A^k \otimes I_B | \psi_i \rangle. \tag{7}$$

In quantum metrology, the QFI and skew information satisfy the following inequality relation as both of them are related to the notion of quantum uncertainty [53]

$$I(\rho, H) \leq F(\rho, H) \leq 2I(\rho, H), \tag{8}$$

from which one gets

$$\text{LQU} \leq \text{QIP} \leq 2\text{LQU}. \tag{9}$$

### 3. Model and Its Solution

This section considers an anisotropic two-qubit Heisenberg XY model subject to an external magnetic field as

$$H = H_{XY} = J(S_1^+ S_2^- + S_1^- S_2^+) + \Delta(S_1^+ S_2^+ + S_1^- S_2^-) + \mathbf{B}(S_1^z + S_2^z), \tag{10}$$

where  $J = (J_x + J_y)/2$  is the spin-spin coupling strength,  $\Delta = (J_x - J_y)/2$  denotes the spin-spin anisotropy parameter, and  $S^\pm = (S^x \pm iS^y)$  denotes the ladder operators with  $S^x = \hbar\sigma^x/2$  and  $S^y = \hbar\sigma^y/2$ . Here, we consider the time-dependent external magnetic field as

$$\mathbf{B} \equiv B(t) = b \cos(\omega t), \tag{11}$$

where  $b$  and  $\omega$  indicate the initial strength and angular frequency of the external magnetic field, respectively.

The time evolution of the system is given by (setting  $\hbar = 1$ )

$$\rho(t) = \exp\left[-i \int_0^t H dt'\right] \rho(0) \exp\left[i \int_0^t H dt'\right], \tag{12}$$

where  $\rho(0)$  is the initial density matrix. Let us assume that the qubits are initially prepared in a Werner state

$$\rho(0) = \frac{1-r}{4} I + r |\Phi\rangle\langle\Phi|, \tag{13}$$

in which  $r$  is the purity factor in the range of  $0 \leq r \leq 1$  and  $|\Phi\rangle = (|00\rangle + |11\rangle)/\sqrt{2}$  is a Bell state. Now, equipped with the Equations (12) and (13), we can get the density matrix of the time-evolved system in the following form

$$\rho(t) = \begin{pmatrix} \vartheta_+ & 0 & 0 & X - iY \\ 0 & \zeta & 0 & 0 \\ 0 & 0 & \zeta & 0 \\ X + iY & 0 & 0 & \vartheta_- \end{pmatrix}, \tag{14}$$

where

$$\begin{aligned} \vartheta_\pm &= \frac{1+r}{4} \pm \frac{rb\Delta\omega t \sin(\omega t) \sin^2(2\mu/\omega)}{2\mu^2}, \\ \zeta &= \frac{1-r}{4}, \\ X &= \frac{r}{2} \left[ 1 - \frac{b^2 \sin^2(\omega t) \sin^2(2\mu/\omega)}{\mu^2} \right], \\ Y &= \frac{rb^2 \sin(\omega t) \sin(2\mu/\omega)}{2\mu}, \end{aligned} \tag{15}$$

with  $\mu = \sqrt{(\Delta\omega t)^2 + b^2 \sin^2(\omega t)}$ . To obtain the explicit expression of LQU, we first compute the elements of Equation (3). It is easy to check that

$$W_{11} = W_{22} = \frac{\chi_-}{4}, \quad W_{33} = \frac{\chi_+}{4} + \frac{(\vartheta_+ - \vartheta_-)^2 - 4(X^2 + Y^2)}{2\alpha}, \tag{16}$$

with

$$\chi_{\pm} = \left(\alpha + 2\sqrt{\zeta}\right)^2 \pm \left(\alpha - 2\sqrt{\zeta}\right)^2,$$

and

$$\alpha = \left(2\sqrt{\vartheta_+\vartheta_- - (X^2 + Y^2)} + \vartheta_+ + \vartheta_-\right)^{1/2}.$$

From the above expressions, the LQU reads

$$\text{LQU}[\rho(t)] = 1 - \max\{W_{11}, W_{33}\}. \tag{17}$$

Similarly, to obtain the explicit form of QIP, one should compute the elements of the matrix  $M$ . Having Equation (7), we can obtain

$$M_{11} = M_{22} = \frac{(\zeta - \eta_+)^2}{\zeta + \eta_+} + \frac{(\zeta - \eta_-)^2}{\zeta + \eta_-}, \quad M_{33} = \frac{4(X^2 + Y^2)}{\vartheta_+ + \vartheta_-}, \tag{18}$$

with

$$\eta_{\pm} = \frac{1}{2} \left( \vartheta_+ + \vartheta_- \pm \sqrt{(\vartheta_+ - \vartheta_-)^2 + 4(X^2 + Y^2)} \right).$$

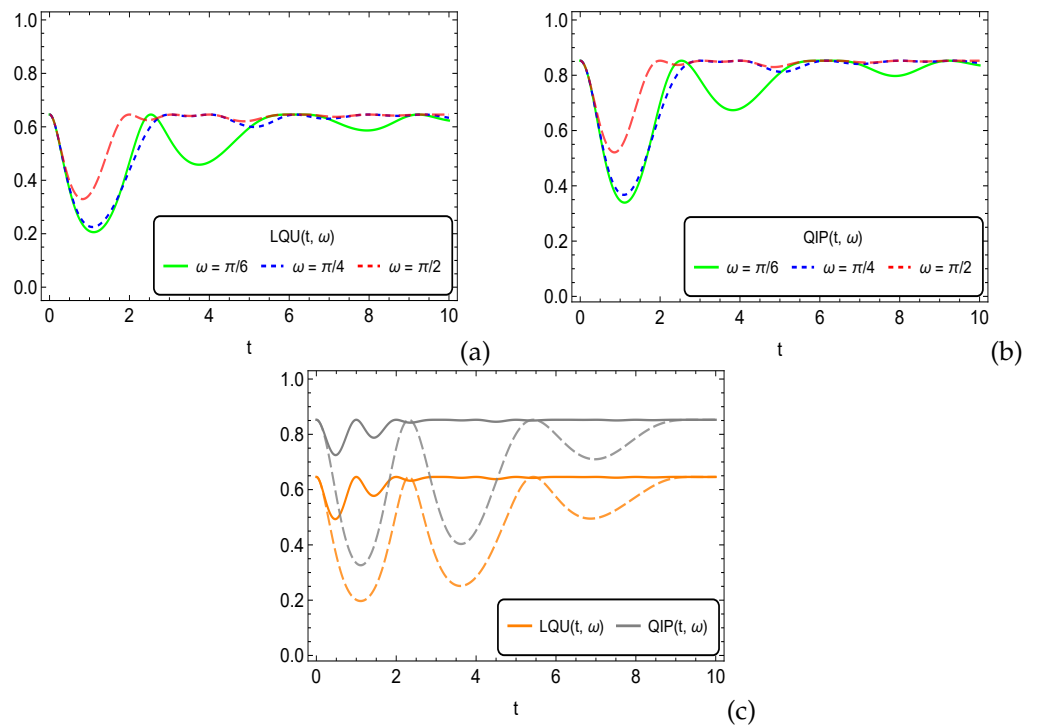
Hence, we have

$$\text{QIP}[\rho(t)] = \min\{M_{11}, M_{33}\}. \tag{19}$$

#### 4. Main Results: Key Discussions

In this section, we provide the main results obtained for the final density matrix given in Equation (14). For the time evolution of quantum correlations and their estimation, we used LQU and QIP measures given in Equations (17) and (19).

In Figure 1, we disclose the dynamics of LQU and QIP in a two-qubit Heisenberg spin chain when influenced by an external magnetic. In the current case, we specifically focus on different fixed values of the angular frequency  $\omega$  of the external magnetic field on the dynamics of the system. Initially, the system remains partially correlated, as we have set  $r = 0.9$ . For each different value of  $\omega$ , the initial non-classical correlations measured by LQU remain the same, while the same can be deduced for the QIP. Besides, the two-qubit correlations suffer a sudden decrease when the interaction between the system and the time-dependent external magnetic field is initiated. However, because of the angular frequency of the external magnetic field, the slopes become reversed after the maximum loss and reach their initial level of quantum correlations. The rest of the dynamical maps of the LQU and QIP quantum correlations either saturate and flow steadily or show revivals with time, depending on the strength of the angular frequency. For example, for the lower  $\omega$  strength, the state achieves its final saturation levels later and so the opposite occurs for the higher values of  $\omega$ . Hence, the final saturation levels and their dynamical maps of LQU and QIP are mainly dependent upon the strength of the angular frequency of the external magnetic field. Finally, in Figure 1c, we set the  $\omega$  parameter to extreme values. For instance, we set  $\omega = \pi$  (solid lines) and  $\pi/10$  (dashed lines), and one can easily deduce that the achievement of the final saturation levels is directly dependent upon the  $\omega$  values. As for  $\omega = \pi/10$ , LQU and QIP suffer from fewer revivals and achieve the initial level of quantum correlations slower. Besides this, the difference between the quantum correlations detection by the LQU and QIP measures is more evident in Figure 1c, however, the fact remains true that both show consistent dynamical maps of quantum correlations in the two-qubit spin chain system.



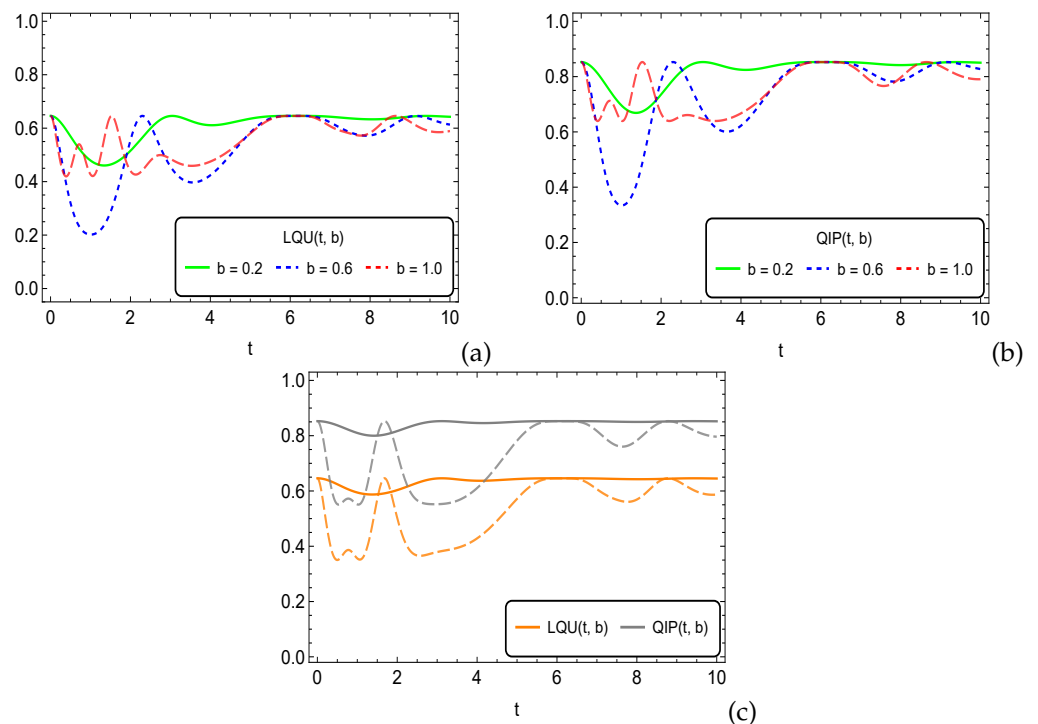
**Figure 1.** LQU and QIP as a function of time versus different values of  $\omega$ . LQU (a) and QIP (b). Graph (c):  $\omega = \pi$  (solid lines) and  $\omega = \pi/10$  (dashed lines). For all plots  $r = 0.9$ ,  $b = 0.5$ , and  $\Delta = 0.5$ .

Figure 2 discloses the time evolution of LQU and QIP measures when primarily characterized by the initial strength of the external magnetic field, namely  $b$ . Initially, the state remains non-maximally correlated and agrees with Figure 1, because we have set the purity factor as  $r = 0.9$ . As the interaction between the system and the external magnetic field is switched on, quantum correlations encoded initially in the state start decaying immediately. However, with time, the reversal of quantum correlations loss occurs and the state again becomes quantum correlated as was encoded initially. The minima of the slopes for both LQU and QIP seem dependent upon the relative values of parameter  $b$ . As one can see for  $b = 1.0$ , the associated minima have an insignificant depth while for  $b = 0.2$  and  $b = 0.6$ , larger minima occur. Nevertheless, LQU and QIP quickly achieve the final saturation levels for the lower initial magnetic field strength  $b = 0.2$  when compared to the higher values of this parameter. Hence, quantum correlations preservation in the considered system can be greatly enhanced by decreasing the initial strength of the magnetic field. Finally, in Figure 2c, we set two extreme values for the initial external magnetic field which are  $b = 0.1$  (solid lines) and  $b = 0.9$  (dashed lines). One can readily deduce that the dynamical maps of LQU and QIP agree. However, the degree of quantum correlations detected by the two measures does not match, whose root can be found in inequality (9).

In Figure 3, we investigate the impact of the anisotropy of the system on the dynamics of quantum correlations in the two-qubit Heisenberg spin chain using LQU and QIP measures. In agreement with Figures 1 and 2, the system remains partially quantum correlated because of setting the purity parameter as  $r = 0.9$ . At the onset, as the interaction between the system and the time-dependent external magnetic field starts, a drop in quantum correlations occurs. The corresponding minimum of the LQU and QIP further depends upon the strength of the anisotropy of the system. For example, for the lower  $\Delta$  values, the LQU and QIP have a larger amplitude. On the other hand, for higher  $\Delta$  magnitudes, the relative amplitude becomes insignificant. This indicates that the drop of quantum correlations at initial interaction times of the Heisenberg spin chain when exposed to an external magnetic field can be readily controlled by enhancing the anisotropy of the

system. Besides, the overall dynamical map of quantum correlations exhibits a revival character but the strength of the revival is encountered to be varied with variation in  $\Delta$ . For lower  $\Delta$  values, the dynamical map of the system exhibits revivals with larger amplitudes and the opposite occurs for higher  $\Delta$  strengths. Finally, for the strong anisotropy parameter  $\Delta$ , quantum correlations quickly reach their final saturation level and the opposite occurs for the weak spin-spin anisotropy strengths. In Figure 3c, we employ two extreme values of the anisotropy strengths, i.e., the weak anisotropy strength  $\Delta = 0.1$  and the strong anisotropy strength  $\Delta = 2.0$ . In the weak anisotropy regime, LQU and QIP achieve very smaller levels while for the higher anisotropy strengths, the higher levels of quantum correlations are achieved. Hence, the degree of quantum correlations at a specific interval of time is largely dependent upon the  $\Delta$  parameter and the optimal degree of them can be obtained at the higher spin-spin anisotropy strength.

We analyze the time-evolution of the quantum correlations functions LQU [Figure 4a] and QIP [Figure 4b] in a two-qubit Heisenberg spin chain system when influenced by an external magnetic field. In particular, we are interested in finding the impact of the purity parameter  $r$  on the degree of preservation of quantum correlations in the mentioned system. Unlike the previous cases, namely Figures 1–3, we obtain different values of initial quantum correlations in the state depending on the parameter  $r$ . As can be seen for  $r = 1$  at  $t = 0$ , the state is maximally correlated/entangled [see Equation (13)], however, for all  $r < 1$ , the state exhibits a partial degree of quantum correlations. Besides, the amplitude of the revivals for higher  $r$  values remains larger while becoming smaller for low  $r$  values. Hence, the revival character of quantum correlations in the given state is also influenced by the purity of the system. It becomes clearer in Figure 4c where a large variation between the degree of quantum correlations and associated revival character has been noticed when the purity of the state is assumed at 0.8 (solid lines) and 0.4 (dashed lines).



**Figure 2.** LQU and QIP as a function of time versus different values of  $b$ . LQU (a) and QIP (b). Graph (c):  $b = 0.1$  (solid lines) and  $b = 0.9$  (dashed lines). For all plots  $r = 0.9$ ,  $\omega = \pi/6$ , and  $\Delta = 0.5$ .

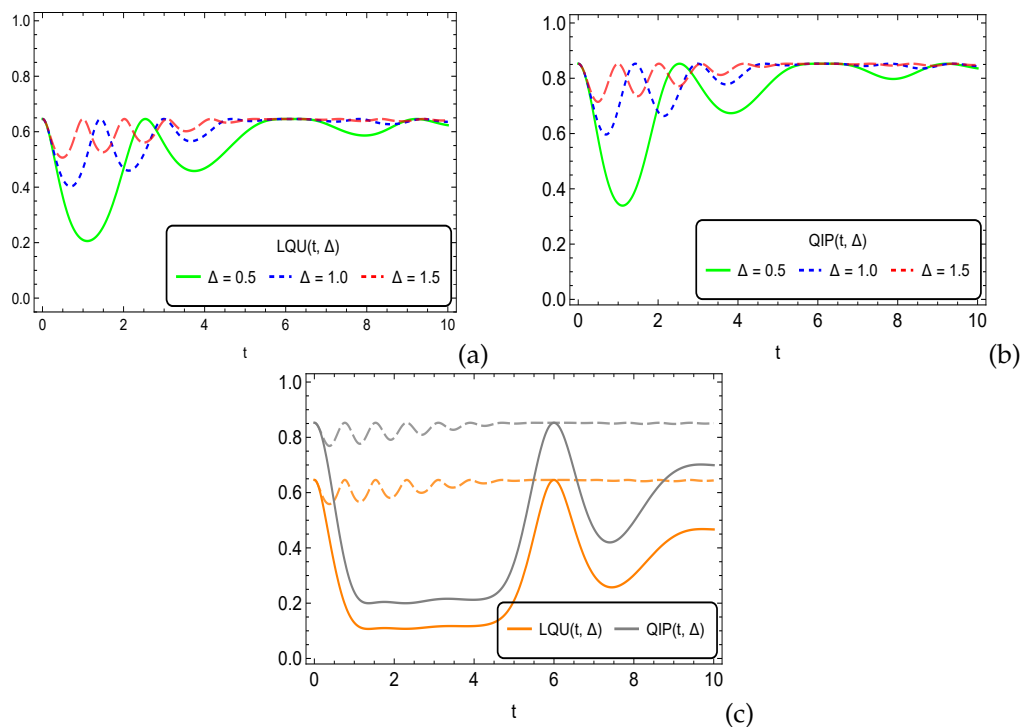


**Figure 3.** LQU and QIP as a function of time versus different values of  $\Delta$ . LQU (a) and QIP (b). Graph (c):  $\Delta = 0.1$  (solid lines) and  $\Delta = 2.0$  (dashed lines). For all plots  $r = 0.9$ ,  $\omega = \pi/6$ , and  $b = 0.5$ .

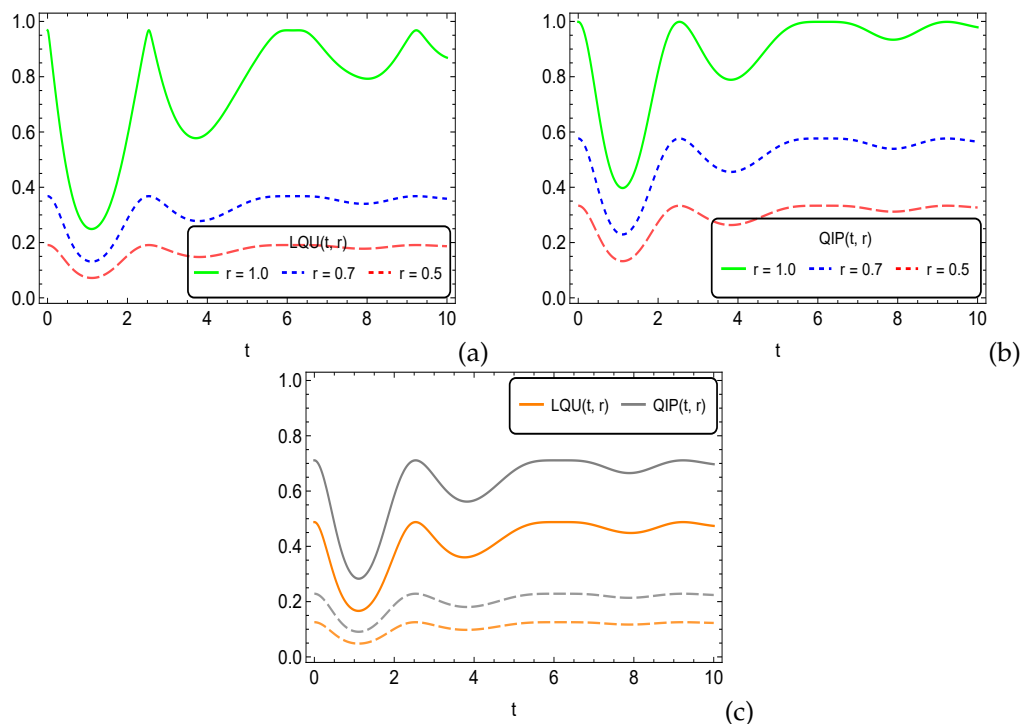


**Figure 4.** LQU and QIP as a function of time versus different values of  $r$ . LQU (a) and QIP (b). Graph (c):  $r = 0.8$  (solid lines) and  $r = 0.4$  (dashed lines). For all plots  $\Delta = 0.5$ ,  $\omega = \pi/6$ , and  $b = 0.5$ .

**5. Analysis of Quantum Correlations with the Bell-Nonlocality Violation Parameter**

The analysis presented in Section 4 can be further expanded by including the Bell parameter, denoted by  $\mathcal{B}(\rho)$ , which provides information about the existence of non-classical correlations in the system described by the density matrix  $\rho$ . A specific expres-

sion to quantify the Bell-nonlocality violation for a quantum state  $\rho$  can be written as  $\mathcal{B}(\rho) = 2\sqrt{M(\rho)}$  [54], where the function  $M(\rho)$  measures the degree of violation of the Bell-nonlocality for a bipartite state. Clearly, when  $M(\rho) > 1$ , we can announce the violation of the Bell inequality. For  $\rho$  that belongs to the class of  $X$ -states, the function  $M(\rho)$  can be expressed in the following form [55]

$$M(\rho) := \max\left\{8(|\rho_{14}|^2 + |\rho_{23}|^2), 4(|\rho_{14}| + |\rho_{23}|)^2 + (\rho_{11} + \rho_{44} - \rho_{22} - \rho_{33})^2\right\}. \quad (20)$$

The Formula (20) allows one to compute a non-classical correlation measure that depends directly on the elements of the density matrix. If we know the dynamical map that represents quantum evolution of our system, we can quantify correlations in the time domain. Consequently, by following the formula for time-evolution of the initial density matrix (14), we can obtain

$$\mathcal{B}[\rho(t)] = 2\sqrt{\max\{8(|X|^2 + |Y|^2), 4(|X|^2 + |Y|^2) + r^2\}}, \quad (21)$$

where  $r$  represents the purity factor and  $X$  and  $Y$  were defined in (15).

The parameter (21) indicates, at an arbitrary time instant  $t$ , the maximum achievable violation of the Bell-CHSH inequality proposed by Clauser, Horne, Shimony and Holt [56].

In Figure 5, we compare the impact of  $\omega$  on the Bell parameter. We have selected an initial state such that  $r = 0.9$ . Then, for three values of the angular frequency of the external magnetic field,  $\omega$ , we follow the nonlocal correlations in the time domain. For  $\omega = \pi/10$ , we witness a significant drop in the value of the Bell parameter, which corresponds to the tendencies presented in Figure 1. On the other hand, for  $\omega = \pi$ , we observe only minor oscillations of the Bell parameter. Ultimately, all plots converge, which means that the initial degree of nonlocality is regained as the evolution continues. The Bell parameter, which is a typical entanglement measure, features the same tendencies as LQU and QIP, which were presented in Figure 1.

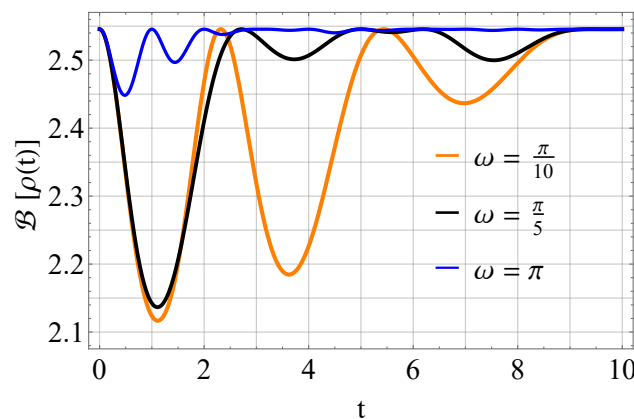


**Figure 5.**  $\mathcal{B}[\rho(t)]$  for three values of  $\omega$ . The other parameters are  $r = 0.9$ ,  $b = 0.5$ , and  $\Delta = 0.5$ .

Moreover, in Figure 6, we present the results obtained for three different values of  $b$ , which represents the initial strength of the magnetic field. As for  $b = 0.1$ , we notice only minor oscillations in the degree of nonlocality, which is consistent with the plots given in Figure 2. For  $b = 0.5$ , we have a deep decline of nonlocality in the initial period. However,  $\mathcal{B}[\rho(t)]$  quickly regains the initial value, and the amplitude of the oscillations tends to decrease later on. When  $b = 0.9$ , the Bell-nonlocality parameter obeys the same tendencies as LQU and QIP presented in Figure 2.

Furthermore, in Figure 7, we investigate how the Bell parameter is affected by the anisotropy of the system denoted by  $\Delta$ . When  $\Delta = 2$ , we have only minor oscillations, which become more significant if we reduce the value of anisotropy to 1. For  $\Delta = 0.1$ , we witness a considerable fall in the Bell-nonlocality. We observe that  $\mathcal{B}[\rho(t)] \approx 2$  for  $t \in (1, 4)$ ,

which means that the system has the least quantum correlations for this period of time (see also Figure 3). However, as the evolution keeps on, the system regains its quantumness.

Eventually, we compare the trajectories of the Bell parameter for three input states in Figure 8. In particular,  $r = 1$  corresponds to the maximally entangled state and  $r = 0.8, 0.4$  represent partially mixed states. We see that when the purity of the input state decreases, the initial value of the non-classical correlations declines but also the oscillations tend to be smaller. The fact that the plot of  $\mathcal{B}[\rho(t)]$  becomes smoother when the purity is reduced is consistent with the observations related to Figure 4.

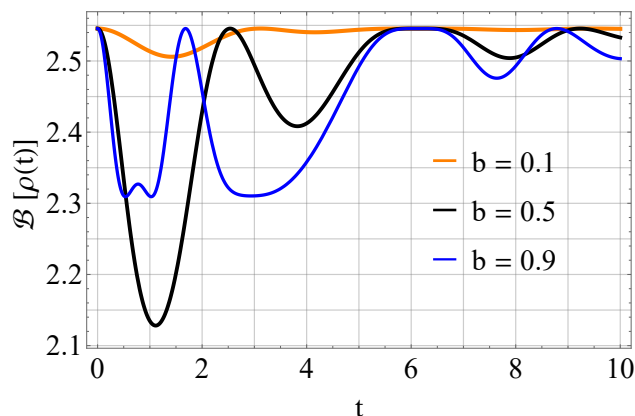


Figure 6.  $\mathcal{B}[\rho(t)]$  for three values of  $b$ . The other parameters are  $r = 0.9, \omega = \pi/6$ , and  $\Delta = 0.5$ .

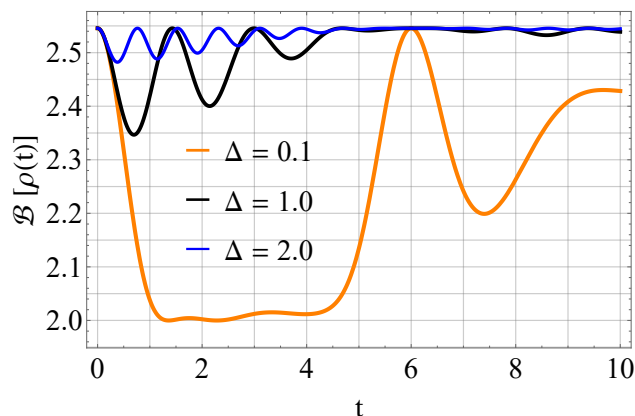


Figure 7.  $\mathcal{B}[\rho(t)]$  for three values of  $\Delta$ . The other parameters are  $r = 0.9, \omega = \pi/6$ , and  $b = 0.5$ .

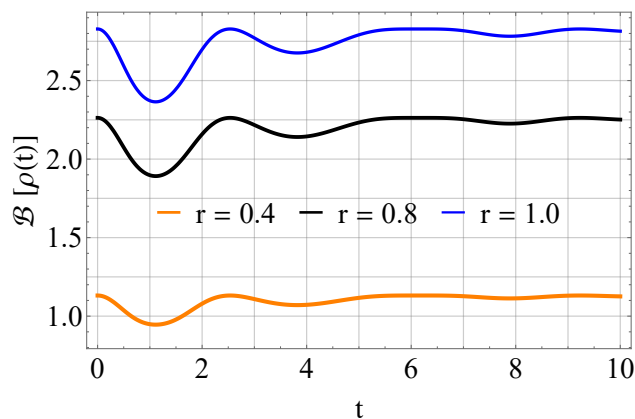


Figure 8.  $\mathcal{B}[\rho(t)]$  for three values of  $r$ . The other parameters are  $\Delta = 0.5, \omega = \pi/6$ , and  $b = 0.5$ .

In most of the previous papers, the Heisenberg spin chains have been found to either completely lose the initially encoded quantum correlation or exhibit some lower levels of it. For example, in Refs. [57–60], quantum coherence and non-classical correlations either face a complete death or achieve lower quantum correlations. In contrast, we presented a two-qubit XY Heisenberg spin chain system which regains the initially encoded quantum correlations after a definite interaction time with the external magnetic field. Moreover, we have analyzed the impact of the angular frequency and the initial strength of the external magnetic field on the dynamics of the system, which has rarely been examined in the studied configurations. Finally, we have illustrated the capacities of the LQU and QIP measures to detect quantum correlations and then we compared them with the Bell-nonlocality violation parameter.

## 6. Conclusions

We have investigated the time-based dynamics of quantum correlations initially encoded in a two-qubit Heisenberg spin chain system when exposed to a time-dependent external magnetic field. We employed LQU and QIP criteria for the measurement of quantum correlations in the considered system. The impact of various parameters of the Heisenberg spin chain system and the initial state, such as spin-spin anisotropy strength, initial strength and angular frequency of external magnetic field, and state's purity on the dynamics of quantum correlations have been studied. Additionally, the findings were confirmed by computing the Bell-nonlocality violation parameter.

We have shown that the current configuration of the Heisenberg spin chain system exposed to the current magnetic field remains a vital resource for the preservation of quantum correlations. However, various parameters of the configuration have been found to influence the preservation degree of quantum correlations. For example, for the lower angular frequency and initial strength of the anisotropy, the associated quantum correlations reach the final saturation level with fewer revivals taking a longer time. For the higher strengths of the forenamed parameters, the dynamical maps of quantum correlations exhibit a greater number of revivals and reach their final maximum saturation levels faster. The purity parameter, on the other hand, regulates the initial as well as the latter levels of quantum correlations preserved in the system. Overall, the quantum correlations preservation in the current Heisenberg spin chain system can be enhanced by the higher values of the state's purity, angular frequency of the external magnetic field, and anisotropy of the system. In other words, by a properly engineered environment, we can control quantum correlations to guarantee that the degree of nonlocality will be regained during the evolution.

**Author Contributions:** Conceptualization, N.Z. and A.U.R.; methodology, N.Z.; software, N.Z., A.U.R., A.C. and S.H. (Saeed Haddadi); validation, all authors; formal analysis, A.U.R., S.H. (Saeed Haddadi) and A.C.; investigation, all authors; resources, A.U.R., A.C. and S.H. (Saeed Haddadi); data curation, S.H. (Soroush Haseli); writing—original draft preparation, A.U.R., A.C. and S.H. (Saeed Haddadi); writing—review and editing, S.H. (Saeed Haddadi), S.H. (Soroush Haseli) and A.C.; supervision, S.H. (Saeed Haddadi); project administration, S.H. (Saeed Haddadi). All authors have read and agreed to the published version of the manuscript.

**Funding:** This research received no external funding.

**Institutional Review Board Statement:** Not applicable.

**Informed Consent Statement:** Not applicable.

**Data Availability Statement:** Not applicable.

**Conflicts of Interest:** The authors declare no conflict of interest.

## Abbreviations

The following abbreviations are used in this manuscript:

LQU	Local quantum uncertainty
MIN	measurement-induced non-locality
QFI	quantum Fisher information
QIP	Quantum interferometric power

## References

- Adesso, G.; Bromley, T.R.; Cianciaruso, M. Measures and applications of quantum correlations. *J. Phys. A Math. Theor.* **2016**, *49*, 473001. [\[CrossRef\]](#)
- Horodecki, R.; Horodecki, P.; Horodecki, M.; Horodecki, K. Quantum entanglement. *Rev. Mod. Phys.* **2009**, *81*, 865. [\[CrossRef\]](#)
- Czerwinski, A. Entanglement characterization by single-photon counting with random noise. *Quantum Inf. Comput.* **2022**, *22*, 1–16. [\[CrossRef\]](#)
- Marletto, C.; Vedral, V. Gravitationally induced entanglement between two massive particles is sufficient evidence of quantum effects in gravity. *Phys. Rev. Lett.* **2017**, *119*, 240402. [\[CrossRef\]](#) [\[PubMed\]](#)
- Martín-Martínez, E.; Brown, E.G.; Donnelly, W.; Kempf, A. Sustainable entanglement production from a quantum field. *Phys. Rev. A* **2013**, *88*, 052310. [\[CrossRef\]](#)
- Roch, N.; Schwartz, M.E.; Motzoi, F.; Macklin, C.; Vijay, R.; Eddins, A.W.; Korotkov, A.N.; Whaley, K.B.; Sarovar, M.; Siddiqi, I. Observation of measurement-induced entanglement and quantum trajectories of remote superconducting qubits. *Phys. Rev. Lett.* **2014**, *112*, 170501. [\[CrossRef\]](#)
- Bloch, I. Quantum coherence and entanglement with ultracold atoms in optical lattices. *Nature* **2008**, *453*, 1016. [\[CrossRef\]](#)
- Cheng W.W.; Gong L.Y.; Shan C.J.; Sheng Y.B.; Zhao S.M. Geometric discord characterize localization transition in the one-dimensional systems. *Eur. Phys. J. D* **2013**, *67*, 121. [\[CrossRef\]](#)
- Qiang W.C.; Zhang H.P.; Zhang L. Geometric global quantum discord of two-qubit X states. *Int. J. Theor. Phys.* **2016**, *55*, 1833 [\[CrossRef\]](#)
- Mohamed, A.B.A.; Khedr, A.N.; Haddadi, S.; Rahman, A.U.; Tammam, M.; Pourkarimi, M.R. Intrinsic decoherence effects on nonclassical correlations in a symmetric spin-orbit model. *Results Phys.* **2022**, *39*, 105693. [\[CrossRef\]](#)
- Luo, S. Using measurement-induced disturbance to characterize correlations as classical or quantum. *Phys. Rev. A* **2008**, *77*, 022301. [\[CrossRef\]](#)
- Mohamed, A.B.A.; Khalil, E.M. Atomic non-locality dynamics of two moving atoms in a hybrid nonlinear system: Concurrence, uncertainty-induced non-locality and Bell inequality. *Opt. Quant. Electron.* **2021**, *53*, 612. [\[CrossRef\]](#)
- Girolami, D.; Tufarelli, T.; Adesso, G. Characterizing nonclassical correlations via local quantum uncertainty. *Phys. Rev. Lett.* **2013**, *110*, 240402. [\[CrossRef\]](#)
- Gibilisco, P.; Girolami, D.; Hansen, F. A unified approach to local quantum uncertainty and interferometric power by metric adjusted skew information. *Entropy* **2021**, *23*, 263. [\[CrossRef\]](#)
- Sbiri, A.; Mansour, M.; Oulouda, Y. Local quantum uncertainty versus negativity through Gisin states. *Int. J. Quantum Inf.* **2021**, *19*, 2150023. [\[CrossRef\]](#)
- Khalid, U.; Jeong, Y.; Shin, H. Measurement-based quantum correlation in mixed-state quantum metrology. *Quantum Inf. Process.* **2018**, *17*, 343. [\[CrossRef\]](#)
- Wu, S.X.; Zhang, Y.; Yu, C.S. Local quantum uncertainty guarantees the measurement precision for two coupled two-level systems in non-Markovian environment. *Ann. Phys.* **2018**, *390*, 71. [\[CrossRef\]](#)
- Lu, X.M.; Yu, S.; Oh, C.H. Robust quantum metrological schemes based on protection of quantum Fisher information. *Nat. Commun.* **2015**, *6*, 7282. [\[CrossRef\]](#)
- Dhar, H.S.; Bera, M.N.; Adesso, G. Characterizing non-Markovianity via quantum interferometric power. *Phys. Rev. A* **2015**, *91*, 032115. [\[CrossRef\]](#)
- Girolami, D.; Souza, A.M.; Giovannetti, V.; Tufarelli, T.; Filgueiras, J.G.; Sarthour, R.S.; Adesso, G. Quantum discord determines the interferometric power of quantum states. *Phys. Rev. Lett.* **2014**, *112*, 210401. [\[CrossRef\]](#)
- Laghmach, R.; El Hadfi, H.; Kaydi, W.; Daoud, M. Dynamic of quantum Fisher information and quantum interferometric power in multipartite coherent states. *Eur. Phys. J. D* **2019**, *73*, 194. [\[CrossRef\]](#)
- Guo, Y.N.; Yang, C.; Tian, Q.L.; Wang G.Y.; Zeng, K. Local quantum uncertainty and interferometric power for a two-qubit system under decoherence channels with memory. *Quantum Inf. Process.* **2019**, *18*, 375. [\[CrossRef\]](#)
- Gessner, M.; Smerzi, A. Statistical speed of quantum states: Generalized quantum Fisher information and Schatten speed. *Phys. Rev. A* **2018**, *97*, 022109. [\[CrossRef\]](#)
- Liu, J.; Yuan, H.; Lu, X.M.; Wang, X. Quantum Fisher information matrix and multiparameter estimation. *J. Phys. A Math. Theor.* **2019**, *53*, 023001. [\[CrossRef\]](#)
- Petz, D.; Ghinea, C. Introduction to quantum Fisher information. In *Quantum Probability and Related Topics*; World Scientific Publishing: Singapore, 2011; pp. 261–281.

26. Frahm, H.; Yu, N.C.; Fowler, M. The integrable XXZ Heisenberg model with arbitrary spin: Construction of the Hamiltonian, the ground-state configuration and conformal properties. *Nucl. Phys. B* **1990**, *336*, 396. [[CrossRef](#)]
27. Santos, L.F. Integrability of a disordered Heisenberg spin-1/2 chain. *J. Phys. A Math. Gen.* **2004**, *37*, 4723. [[CrossRef](#)]
28. Essler, F.H.; Piroli, L. Integrability of one-dimensional Lindbladians from operator-space fragmentation. *Phys. Rev. E* **2020**, *102*, 062210. [[CrossRef](#)]
29. Heisenberg, W. Zur theorie des ferromagnetismus. *Z. Physik* **1928**, *49*, 619. [[CrossRef](#)]
30. Serban, D.; Staudacher, M. Planar  $\mathcal{N} = 4$  gauge theory and the Inozemtsev long range spin chain. *JHEP06* **2004**, *2004*, 001. [[CrossRef](#)]
31. Hernandez, R.; Lopez, E. The  $SU(3)$  spin chain sigma model and string theory. *JHEP04* **2004**, *2004*, 052. [[CrossRef](#)]
32. Lovesey, S.W.; Balcar, E. A theory of the time-dependent properties of Heisenberg spin chains at infinite temperature. *J. Phys. Condens. Matter.* **1994**, *6*, 1253. [[CrossRef](#)]
33. Arian Zad, H.; Ananikian, N. Phase transitions and thermal entanglement of the distorted Ising–Heisenberg spin chain: Topology of multiple-spin exchange interactions in spin ladders. *J. Phys. Condens. Matter.* **2017**, *29*, 455402. [[CrossRef](#)]
34. Haddadi, S.; Pourkarimi, M.R.; Akhound, A.; Ghominejad, M. Thermal quantum correlations in a two-dimensional spin star model. *Mod. Phys. Lett. A* **2019**, *34*, 1950175. [[CrossRef](#)]
35. Hu, M.L.; Gao, Y.Y.; Fan, H. Steered quantum coherence as a signature of quantum phase transitions in spin chains. *Phys. Rev. A* **2020**, *101*, 032305. [[CrossRef](#)]
36. Khedif, Y.; Daoud, M. Thermal quantum correlations in the two-qubit Heisenberg XYZ spin chain with Dzyaloshinskii–Moriya interaction. *Mod. Phys. Lett. A* **2021**, *36*, 2150074. [[CrossRef](#)]
37. Khedif, Y.; Haddadi, S.; Pourkarimi, M.R.; Daoud, M. Thermal correlations and entropic uncertainty in a two-spin system under DM and KSEA interactions. *Mod. Phys. Lett. A* **2021**, *36*, 2150209. [[CrossRef](#)]
38. Ait Chlih, A.; Habiballah, N.; Nassik, M. Dynamics of quantum correlations under intrinsic decoherence in a Heisenberg spin chain model with Dzyaloshinskii–Moriya interaction. *Quantum Inf. Process.* **2021**, *20*, 92. [[CrossRef](#)]
39. Oumennana, M.; Rahman, A.U.; Mansour, M. Quantum coherence versus non-classical correlations in XXZ spin-chain under Dzyaloshinsky–Moriya (DM) and KSEA interactions. *Appl. Phys. B* **2022**, *128*, 162. [[CrossRef](#)]
40. Benabdallah, F.; Anouz, K.E.; Daoud, M. Toward the relationship between local quantum Fisher information and local quantum uncertainty in the presence of intrinsic decoherence. *Eur. Phys. J. Plus* **2022**, *137*, 548. [[CrossRef](#)]
41. Benabdallah, F.; Anouz, K.E.; Strecka, J.; Daoud, M. Thermal non-classical correlation via skew information, quantum Fisher information, and quantum teleportation of a spin-1/2 Heisenberg trimer system. *Eur. Phys. J. Plus* **2022**, *137*, 1096. [[CrossRef](#)]
42. Haseli, S. Local quantum Fisher information and local quantum uncertainty in two-qubit Heisenberg XYZ chain with Dzyaloshinskii–Moriya interactions. *Laser Phys.* **2020**, *30*, 105203. [[CrossRef](#)]
43. Khedif, Y.; Haddadi, S.; Daoud, M.; Dolatkah, H.; Pourkarimi, M.R. Non-classical correlations in a Heisenberg spin model with Heitler–London approach. *Quantum Inf. Process.* **2022**, *21*, 235. [[CrossRef](#)]
44. Malvezzi, A.L.; Karpat, G.; Çakmak, B.; Fanchini, F.F.; Debarba, T.; Vianna, R.O. Quantum correlations and coherence in spin-1 Heisenberg chains. *Phys. Rev. B* **2016**, *93*, 184428. [[CrossRef](#)]
45. Shi, W.N.; Ming, F.; Wang, D.; Ye, L. Entropic uncertainty relations in the spin-1 Heisenberg model. *Quantum Inf. Process.* **2019**, *18*, 70. [[CrossRef](#)]
46. Werlang, T.; Trippé, C.; Ribeiro, G.A.P.; Rigolin, G. Quantum correlations in spin chains at finite temperatures and quantum phase transitions. *Phys. Rev. Lett.* **2010**, *105*, 095702. [[CrossRef](#)]
47. Zheng, Y.; Mao, Z.; Zhou, B. Thermal quantum correlations of a spin-1/2 Ising–Heisenberg diamond chain with Dzyaloshinskii–Moriya interaction. *Chinese Phys. B* **2018**, *27*, 090306. [[CrossRef](#)]
48. Yurischev, M.A. On the quantum correlations in two-qubit XYZ spin chains with Dzyaloshinsky–Moriya and Kaplan–Shekhtman–Entin-Wohlman–Aharony interactions. *Quantum Inf. Process.* **2020**, *19*, 336. [[CrossRef](#)]
49. Benabdallah, F.; Rahman, A.U.; Haddadi, S.; Daoud, M. Long-time protection of thermal correlations in a hybrid-spin system under random telegraph noise. *Phys. Rev. E* **2022**, *106*, 034122. [[CrossRef](#)]
50. Alenezi, M.; Zidan, N.; Alhashash, A.; Rahman, A.U. Quantum Fisher Information Dynamics in the Presence of Intrinsic Decoherence. *Int. J. Theor. Phys.* **2022**, *61*, 153. [[CrossRef](#)]
51. Braunstein, S.L.; Caves, C.M. Statistical distance and the geometry of quantum states. *Phys. Rev. Lett.* **1994**, *72*, 3439. [[CrossRef](#)]
52. Elghaayda, S.; Dahbi, Z.; Mansour, M. Local quantum uncertainty and local quantum Fisher information in two-coupled double quantum dots. *Opt. Quant. Electron.* **2022**, *54*, 419. [[CrossRef](#)]
53. Luo, S. Wigner–Yanase skew information versus quantum Fisher information. *Proc. Am. Math. Soc.* **2003**, *132*, 885. [[CrossRef](#)]
54. Horodecki, R.; Horodecki, P.; Horodecki, M. Violating Bell inequality by mixed spin-1/2 states: Necessary and sufficient condition. *Phys. Lett. A* **1995**, *200*, 340. [[CrossRef](#)]
55. Hu, M.L. Relations between entanglement, bell-inequality violation and teleportation fidelity for the two-qubit X states. *Quant. Inf. Process.* **2013**, *12*, 229. [[CrossRef](#)]
56. Clauser, J.F.; Horne, M.A.; Shimony, A.; Holt, R.A. Proposed experiment to test local hidden-variable theories. *Phys. Rev. Lett.* **1969**, *23*, 880. [[CrossRef](#)]
57. Haseli, S.; Haddadi, S.; Pourkarimi, M.R. Entropic uncertainty lower bound for a two-qubit system coupled to a spin chain with Dzyaloshinskii–Moriya interaction. *Opt. Quant. Electron.* **2020**, *52*, 465. [[CrossRef](#)]

58. Hashem, M.; Mohamed, A.B.A.; Haddadi, S.; Khedif, Y.; Pourkarimi, M.R.; Daoud, M. Bell nonlocality, entanglement, and entropic uncertainty in a Heisenberg model under intrinsic decoherence: DM and KSEA interplay effects. *Appl. Phys. B* **2022**, *128*, 87. [[CrossRef](#)]
59. Benabdallah, F.; Haddadi, S.; Arian Zad, H.; Pourkarimi, M.R.; Daoud, M.; Ananikian, N. Pairwise quantum criteria and teleportation in a spin square complex. *Sci. Rep.* **2022**, *12*, 6406. [[CrossRef](#)]
60. Haddadi, S.; Pourkarimi, M.R.; Khedif, Y.; Daoud, M. Tripartite measurement uncertainty in a Heisenberg XXZ model. *Eur. Phys. J. Plus* **2022**, *137*, 66. [[CrossRef](#)]

**Disclaimer/Publisher's Note:** The statements, opinions and data contained in all publications are solely those of the individual author(s) and contributor(s) and not of MDPI and/or the editor(s). MDPI and/or the editor(s) disclaim responsibility for any injury to people or property resulting from any ideas, methods, instructions or products referred to in the content.